Structural Engineering and Mechanics, Vol. 42, No. 2 (2012) 229-245
DOI: http://dx.doi.org/10.12989/sem.2012.42.2.229

Estimation of bridge displacement responses using FBG sensors and theoretical mode shapes

Soobong Shin[1], Sun-Ung Lee[1], Yuhee Kim[1] and Nam-Sik Kim*[2]

[1]*Department of Civil Engineering, Inha University, Incheon, Korea*
[2]*Department of Civil and Environmental Engineering, Pusan National University, Busan, Korea*

(Received January 10, 2011, Revised February 20, 2012, Accepted March 18, 2012)

Abstract. Bridge vibration displacements have been directly measured by LVDTs (Linear Variable Differential Transformers) or laser equipment and have also been indirectly estimated by an algorithm of integrating measured acceleration. However, LVDT measurement cannot be applied for a bridge crossing over a river or channel and the laser technique cannot be applied when the weather condition is poor. Also, double integration of accelerations may cause serious numerical deviation if the initial condition or a regression process is not carefully controlled. This paper presents an algorithm of estimating bridge vibration displacements using vibration strains measured by FBG (Fiber Bragg Grating) sensors and theoretical mode shapes of a simply supported beam. Since theoretically defined mode shapes are applied, even high modes can be used regardless of the quality of the measured data. In the proposed algorithm, the number of theoretical modes is limited by the number of sensors used for a field test to prevent a mathematical rank deficiency from occurring in computing vibration displacements.89The proposed algorithm has been applied to various types of bridges and its efficacy has been verified. The closeness of the estimated vibration displacements to measured ones has been evaluated by computing the correlation coefficient and by comparing FRFs (Frequency Response Functions) and the maximum displacements.

Keywords: vibration displacement, FBG sensors, theoretical mode shapes, correlation coefficient, FRF

1. Introduction

Bridge vibration displacements provide useful information for bridge assessment and health monitoring if they can be measured or estimated (Bhagwat *et al*. 2011, Brownjohn *et al*. 2004, Chan *et al*. 2009, Inaudi *et al*. 1998, Liu *et al*. 2011). Vibration displacements are usually less influenced by high mode vibrations than by accelerations and strains. The impact factor for a bridge structure is more reliably computed by the ratio of maximum vibration displacement to static displacement than by comparing maximum vibration strains to static strains (AASHTO 2008).

Conventionally, displacements have been directly measured by LVDTs (Linear Variable Differential Transformers) which usually require temporary supporting structures (Park *et al*. 2005). Since it is almost impossible to apply this method for tall bridges and bridges crossing over a river or channel (Whiteman *et al.* 2002), laser techniques have been applied instead in some cases by measuring the movement of a target attached to a bridge (Lee *et al*. 2006, Lassif *et al*. 2005). The

*Corresponding author, Associate Professor, E-mail: nskim@pusan.ac.kr

accuracy of the laser method is usually within a tolerable range but the equipment is expensive and inconvenient to use in the field (Chan *et al*. 2009). The laser technique cannot measure a target displacement correctly when the weather condition is poor due to fog or rain. Also, the laser technique cannot measure displacements of multiple locations concurrently. Methods using GPS (Global Positioning System) systems and digital cameras have also been developed and applied in recent years but these approaches still lack relative accuracy (Meng *et al*. 2007).

Indirect methods of estimating dynamic displacements can be classified into two categories depending on the type of measurement sources; accelerations (Gindy *et al*. 2008) and strains (Foss *et al*. 1995, Kang *et al*. 2007, Kirby *et al*. 1997, Todd *et al*. 1999). When acceleration data is used to estimate displacements, double integration of acceleration is required to compute displacement with two initial conditions (Jiang *et al*. 2002). However, in reality, the vibration response derived from the measured acceleration may be always biased. Since the bias error is serious in actual applications, the estimation error is highly dependent on the appropriateness of the bias correction and the error in the initial conditions (Park *et al*. 2005). To escape from this indispensible bias error related to the integration of state response, Jung and Kim (2006) proposed a transformation method of computing displacements from measured acceleration in the post-process. The method has been successfully applied to field data but the results were still highly dependent on the selection of the starting and ending time points in the measured acceleration data. Some methods of computing displacements using measured strains have been also introduced based on the Euler-Bernoulli beam theory but their applications were limited to simulation or laboratory studies on simple span beams (Shin *et al*. 2007, Kang *et al*. 2007). Chang *et al*. (2009) also proposed a mode decomposition method of using measured dynamic strain signals but the algorithm is relatively complicated and highly dependent on the accuracy of the modal data identified from the measured response. Many previous researchers (Davis *et al*. 1994, Todd *et al*. 2000, Vohra *et al*. 2000, Vurpillot *et al*. 1996) have also carried out the applications of fiber optic Bragg-grating (FBG) sensors to estimate the structural responses indirectly.

This current paper presents an algorithm of estimating bridge vibration displacements using vibration strains measured by FBG sensors and theoretical mode shapes of a simply supported beam. Since theoretically defined mode shapes are applied, even theoretical high modes can be used regardless of the quality of measured field data. In applying the proposed algorithm, the number of theoretical modes is limited by the number of sensors used for the field measurements to prevent the mathematical rank deficiency from occurring in computing vibration displacements.

To verify the efficiency of the proposed algorithm, the algorithm has been applied in field tests on various types of bridges including a bridge for Maglev trains, a self-anchored suspension bridge with three continuous spans, and a multi-girder simple span bridge. The effects of the number of sensors and thus the number of theoretical modes on the accuracy of the estimated results have been investigated with a field test data from the self-anchored suspension bridge. The closeness of the estimated results to the actual displacements has been evaluated by computing the correlation coefficient and by comparing FRFs (Frequency Response Functions) and the maximum displacements.

2. Algorithm for estimating vibration displacement from measured strains

The vibration displacement y_i at location x_i in the longitudinal direction of a structure can be

expressed by the modal superposition of separated variables as Eq. (1).

$$\{y_i(t)\}_{m\times 1} = \{y(x_i,t)\}_{m\times 1} = [\phi_{ij}]_{m\times n}\{q_j(t)\}_{n\times 1} \tag{1}$$

where ϕ_{ij}, and $q_j(t)$ = the modal displacement at location x_i and the generalized coordinate of the jth mode at time t, respectively, while m and n = the number of measuring points and the number of modes, respectively. The number of measuring points m has the same meaning as the number of sensors used for the measurements herein.

From the Euler-Bernoulli beam theoy, strain ε_{i,y_c} at location x_i in the longitudinal direction and at distance y_c from the neutral axis can be related to the curvature y'' by Eq. (2).

$$\{\varepsilon_{i,y_c}(t)\}_{m\times 1} = y_c\{y''(x_i,t)\}_{m\times 1} = y_c[\phi''_{ij}]_{m\times n}\{q_j(t)\}_{n\times 1} \tag{2}$$

where ϕ''_{ij} = curvature of modal displacement ϕ_{ij}.

Since the curvature matrix $[\phi''_{ij}]_{m\times n}$ is not symmetric, a least squared solution can be obtained for $\{q_j(t)\}_{n\times 1}$ by Eq. (3).

$$\{q_j(t)\}_{n\times 1} = \frac{1}{y_c}[[\phi''_{ij}]^T[\phi''_{ij}]]^{-1}_{n\times n}[\phi''_{ij}]^T\{\varepsilon_{i,y_c}(t)\}_{m\times 1} \tag{3}$$

By inserting $\{q_j(t)\}_{n\times 1}$ of Eq. (3) into Eq. (1), the relationship between vibration displacements and strains can be finally derived as Eq. (4).

$$\{y_i(t)\}_{m\times 1} = \frac{1}{y_c}[\phi_{ij}]_{m\times n}[[\phi''_{ij}]^T[\phi''_{ij}]]^{-1}_{n\times n}[\phi''_{ij}]^T_{n\times m}\{\varepsilon_{i,y_c}(t)\}_{m\times 1} \tag{4}$$

The vibration displacements of Eq. (4) are estimated by Eq. (1) after evaluating the general coordinates of $\{q_j(t)\}_{n\times 1}$ for each mode by Eq. (3). Since the proposed algorithm applies theoretical mode shapes, the mode shape matrix $[\phi_{ij}]$ can be extensively obtained depending on the required locations for estimating vibration displacements which may not be simply limited to the locations of measuring strains. In that case, the size of mode shape matrix $[\phi_{ij}]$ should be also changed according to the number of required locations. However, the current research limits the locations of estimating vibration displacements only to the same locations of measuring strains. The estimation of vibration displacements at arbitrary locations is out of the current research scope.

In order to obtain a proper solution for $\{q_j(t)\}_{n\times 1}$ from the system of equations of Eq. (2), the following criterion of Eq. (5) should be satisfied.

$$m \geq n \tag{5}$$

Eq. (5) indicates that the number of sensors used for the measurements must be larger or at least equal to the number of modes applied. In other words, the number of theoretical modes used for the estimation must be smaller or at most equal to the number of sensors used for the experiment. If this criterion of Eq. (5) is not met, the system of equations of Eq. (2) will be under-determined with rank deficiency so that multiple solutions may be obtained. Because using more sensors and thus more modes may result in a better estimation, it may be preferable to set the number of modes equal to the number of sensors by $n = m$. In this case, the vibration displacements can be computed directly by Eq. (6) at the locations of measured strains.

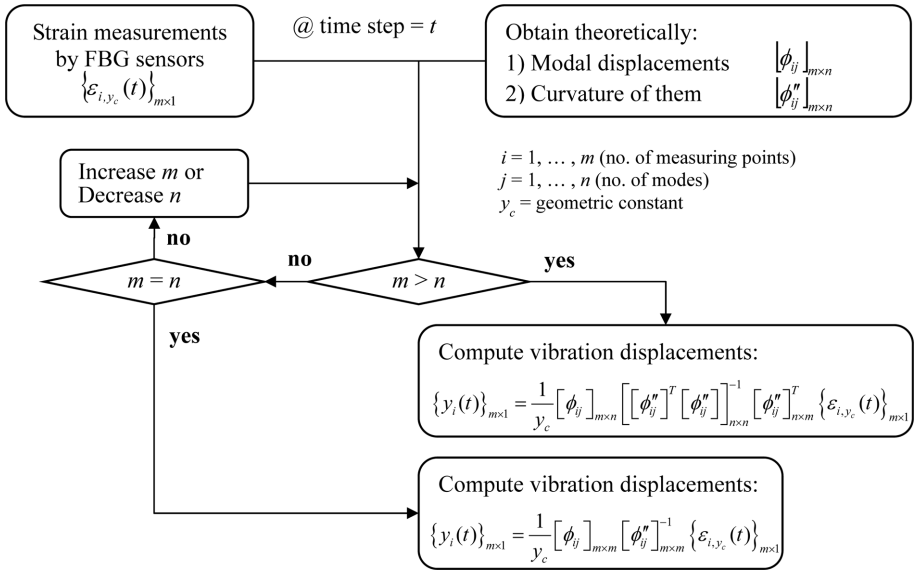

Fig. 1 Flow of computing vibration displacements from measured strains and theoretical mode shapes

$$\{y_i(t)\}_{m\times1} = \frac{1}{y_c}[\phi_{ij}]_{m\times m}[\phi''_{ij}]^T_{m\times m}\{\varepsilon_{i,y_c}(t)\}_{m\times1} \tag{6}$$

Since the Euler-Bernoulli beam theory cannot be exactly satisfied in actual bridge sections, it is suggested in the current study to obtain the geometric constant y_c from a field test data instead of using a theoretical value. Therefore, it is required to carry out a controlled field test to determine the value of y_c as a scale factor before the proposed algorithm is applied to estimate vibration displacements.

Since the proposed algorithm adopts the theoretical mode shape ϕ_{ij} and its corresponding curvature ϕ''_{ij} from the Euler-Bernoulli beam theory, the following equations of Eq. (7) can be directly applied to Eq. (4) or Eq. (6) for the case of a simply supported beam.

$$\phi_{ij} = \sin\frac{j\pi x_i}{L}, \quad \phi''_{ij} = -\left(\frac{j\pi}{L}\right)^2 \sin\frac{j\pi x_i}{L} = -\left(\frac{j\pi}{L}\right)^2 \phi_{ij} \tag{7}$$

where L = length of the beam.

The process of computing vibration displacements suggested in the paper is schematically summarized in Fig. 1.

3. Experimental verification

3.1 Application to a single span Maglev bridge

The proposed algorithm has been examined with field test data obtained from a bridge for Maglev trains as shown in Fig. 2. FBG sensors were placed at the bottom of the girder bridge. Two LVDTs were also located at the bottom of the middle span as illustrated in the figure. Average response

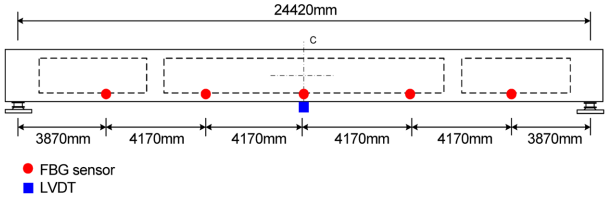

(a) Location of sensors

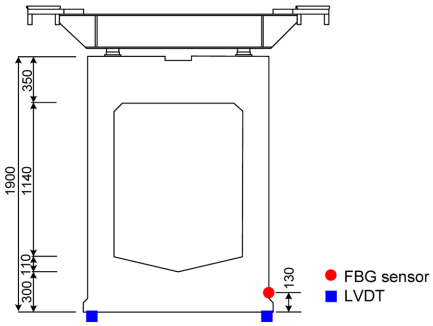

(b) Section of a girder bridge

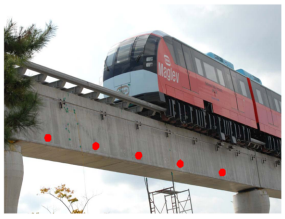

(c) View of a Maglev train on a girder bridge

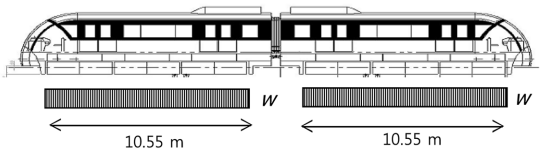

w = 28 kN/m for maximum live load

(d) Maglev train

Fig. 2 Field test on a bridge for Maglev train

from two LVDTs was used as the vertical vibration displacement of the girder bridge. The train ran at various speeds from 10 km/hr to 50 km/hr over the girder bridge for the tests.

The geometric constant y_c in Eq. (4) was determined as 52.68 cm from the case of the vehicle speed of 10 km/hr. By using y_c determined from the reference case of 10 km/hr speed, the vibration displacements were computed and compared with those measured from LVDTs at the speeds of 30 km/hr and 50 km/hr respectively in Fig. 3. With the exception of some minor discrepancies when the train passed over the midspan, the estimated displacements are in relatively good agreement with the measured data.

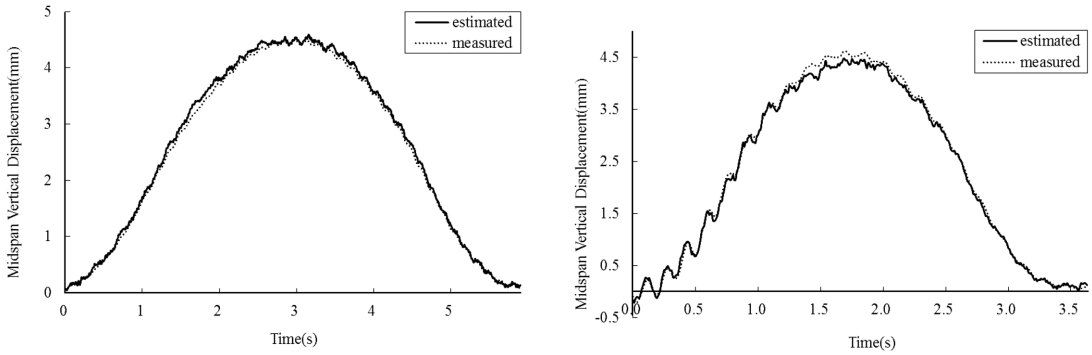

(a) 30km/hr (b) 50km/hr

Fig. 3 Comparison of displacements at the midspan of a bridge for Maglev train

Table 1 Comparison of estimated and measured displacements of a bridge for Maglev train at different speeds

Velocity (km/hr)	Correlation coefficient	Maximum displacement @ midspan		
		u_{est} (mm)	u_{meas} (mm)	Difference (%)
10	0.9997	45.025	44.505	1.17
20	0.9997	45.759	44.790	2.16
30	0.9997	45.929	44.980	2.11
40	0.9994	43.731	44.970	2.76
50	0.9995	44.744	46.125	2.99

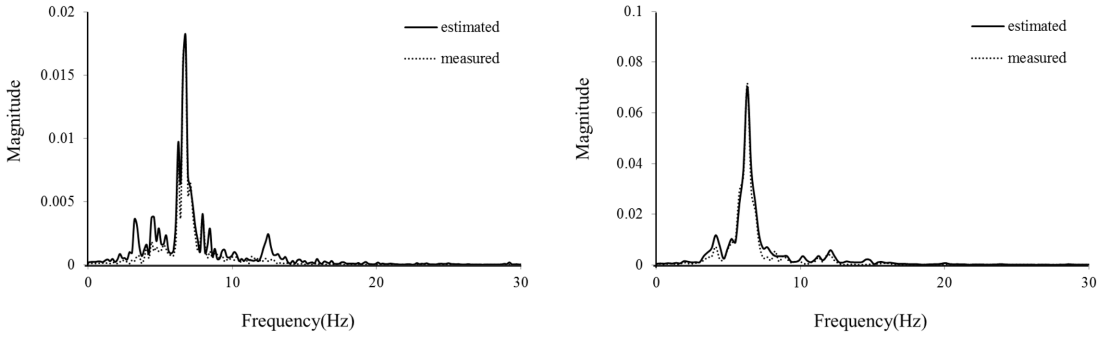

(a) 30km/h (b)50km/h

Fig. 4 Comparison of FRFs of estimated and measured displacements of a bridge for Maglev train at different speeds

Table 1 confirms the good match between estimated and measured vibration displacements at the midspan by the correlation coefficients and the difference in maximum displacements. Fig. 4 compares FRFs computed from the estimated and the measured vibration displacements and shows good agreement even in the frequency domain with the same peak frequencies.

3.2 Application to a self-anchored suspension bridge

The algorithm has also been applied to a self-anchored three-continuous span suspension bridge in Korea. Fifteen FBG strain sensors were equally spaced only in the main span as shown in Fig. 5. Vibration at the center of the main span of the suspension bridge has been estimated by the modal superposition of vibration modes of a simply supported beam representing only the main span of the bridge.

The geometric constant $y_r = (\pi/L)^2 y_c$ was determined from Fig. 6 when a truck ran at the speed of 5 km/hr. The determined value of y_c has been used for all the other tested cases in the current study. As demonstrated in Fig. 6, the geometric constant y_r could be determined with the values in the non-fluctuating region where a truck passed over the middle span. Based on the experiences

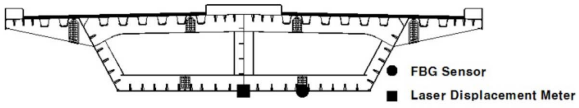

(a) Cross section of the bridge

(b) View of a truck on the bridge

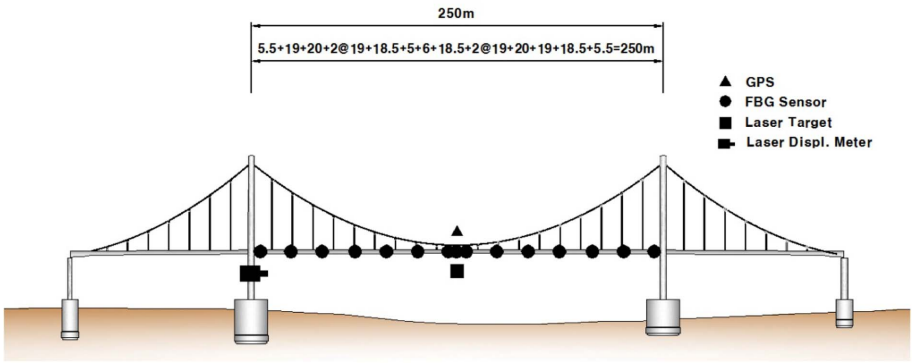

(c) Locations of FBG sensors and laser target in the bridge

Fig. 5 View of Sorok suspension bridge and the locations of sensors

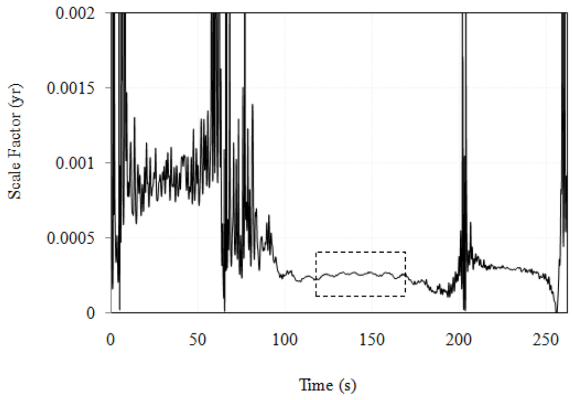

Fig. 6 Determination of y_r from the field test (5 km/hr)

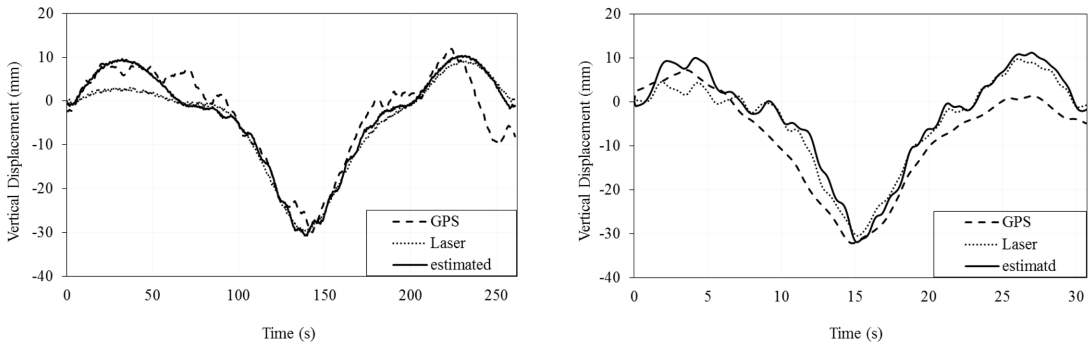

(a) 5km/hr (b) 60km/hr

Fig. 7 Comparison of estimated and measured displacements at the center of the main span at different truck speeds

from series of field tests, it is recommended to determine the geometric constant by a pseudo-static test with a truck running at a low speed. However, after the geometric constant is determined once from a controlled field test, the determined value can be kept using afterwards.

To validate the estimated displacements, the vibration displacements at the center of the main span were measured directly by the laser displacement meter and also by the differential GPS system and these results are compared in Fig. 7 for the speeds of 5 km/hr and 60 km/hr, respectively.

The figures in Fig. 7 were drawn for the period from when a truck entered to when it exited the bridge. Overall, the estimated vibration displacements are closer to the vibration displacements measured by the laser displacement meter than to those measured by the differential GPS system. However, the relatively large gap between the estimated and the measured vibration displacements measured by the laser displacement meter can be observed when the trucks were on the approaching side of the suspension bridge. It is assumed that this phenomenon might be due to the rotation of the laser displacement meter itself while the truck was on the approaching side. The laser displacement meter was located at the top of a crossbeam of the left pylon as shown in Fig. 5(c).

Table 2 summarizes the computed correlation coefficients between the estimated vibration displacements and the vibration displacements measured by the laser displacement meter at various

Table 2 Comparison of estimated and measured displacements of Sorok bridge at various truck speeds

Velocity (km/hr)	Correlation coefficient ($u_{est} - u_{laser}$)		Max. Displacement @ midspan				
	Whole	Mid only	u_{est} (mm)	u_{laser} (mm)	Diff. (%)	u_{GPS} (mm)	Diff. (%)
5	0.9840	0.9946	30.666	29.879	2.63	29.915	2.51
10	0.9865	0.9930	30.642	29.249	4.77	32.020	4.30
20	0.9864	0.9949	29.669	29.751	0.28	32.412	8.46
50	0.9870	0.9942	31.909	30.503	4.61	25.049	27.38
60	0.9850	0.9846	31.890	30.454	4.72	32.137	0.77
70	0.9879	0.9943	31.524	30.021	5.01	32.365	2.60

truck speeds. The correlation coefficients were computed with the displacement data in the whole range and also with the data only when the truck was in the main span where all the FBG sensors were placed. When vibration displacements are compared within the main span, the correlation between the estimated and measured vibration displacements is improved. Table 2 also compares the maximum displacements at the midspan at various truck speeds and confirms good agreements. The maximum displacements by the differential GPS method are also compared in the same table and show relatively reliable results with the exception of the case of the speed of 50 km/hr. In Table 2, u_{est}, u_{laser} and u_{GPS} represent maximum values of estimated vibration displacement, measured displacement by the laser displacement meter, and measured displacement by the GPS system, respectively.

FRFs of the estimated vibration displacements and the vibration displacements measured by the laser displacement meter obtained at the center of the main span are compared in Figs. 8 and 9. Fig. 8 is drawn with the displacement data of the whole range while Fig. 9 is drawn with the displacements only when trucks were on the main span. FRFs for the speed of 60 km/h match each other well in the frequency domain in both figures. However, for the low speed of 5 km/h, some gaps in the magnitude of FRFs are observed.

The effect of the number of sensors and thus the number of theoretical modes used for the estimation of the estimation accuracy has been investigated in Fig. 10. As the number of FBG strain

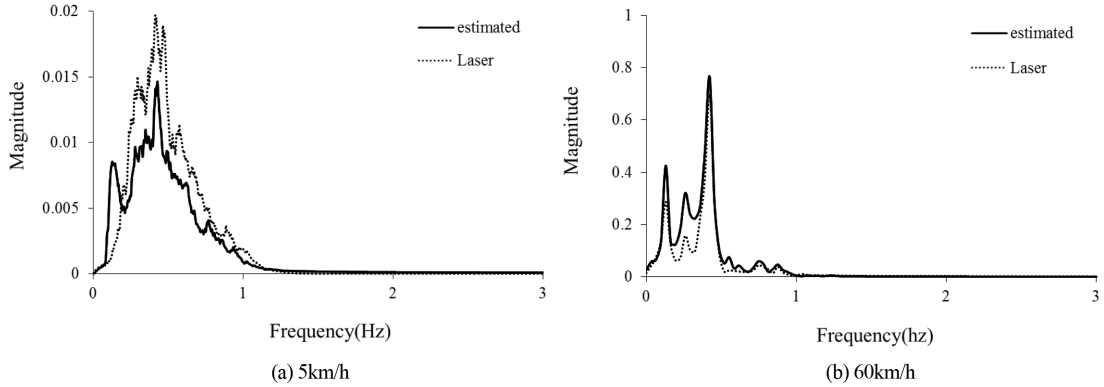

Fig. 8 Comparison of FRFs of estimated and measured displacements at the center of a bridge at different speeds (with data of the whole range)

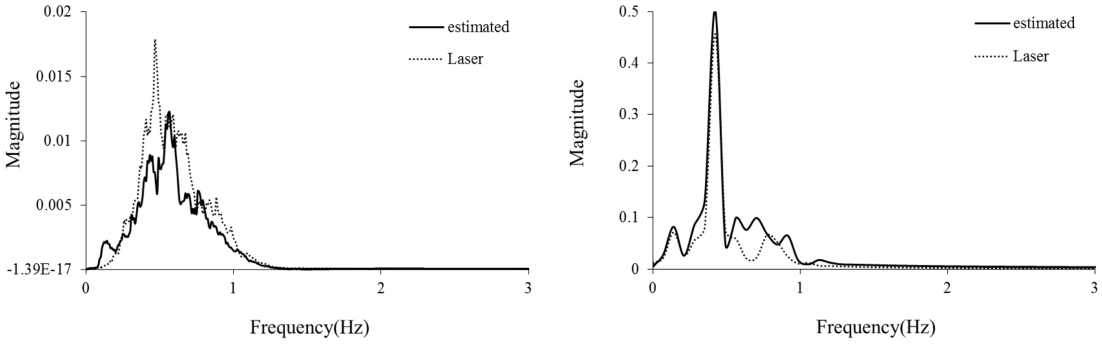

(a) 5km/h(center) (b) 60km/h(center)

Fig. 9 Comparison of FRFs of estimated and measured displacements at the center of a bridge at different speeds (with data only when trucks were in the main span)

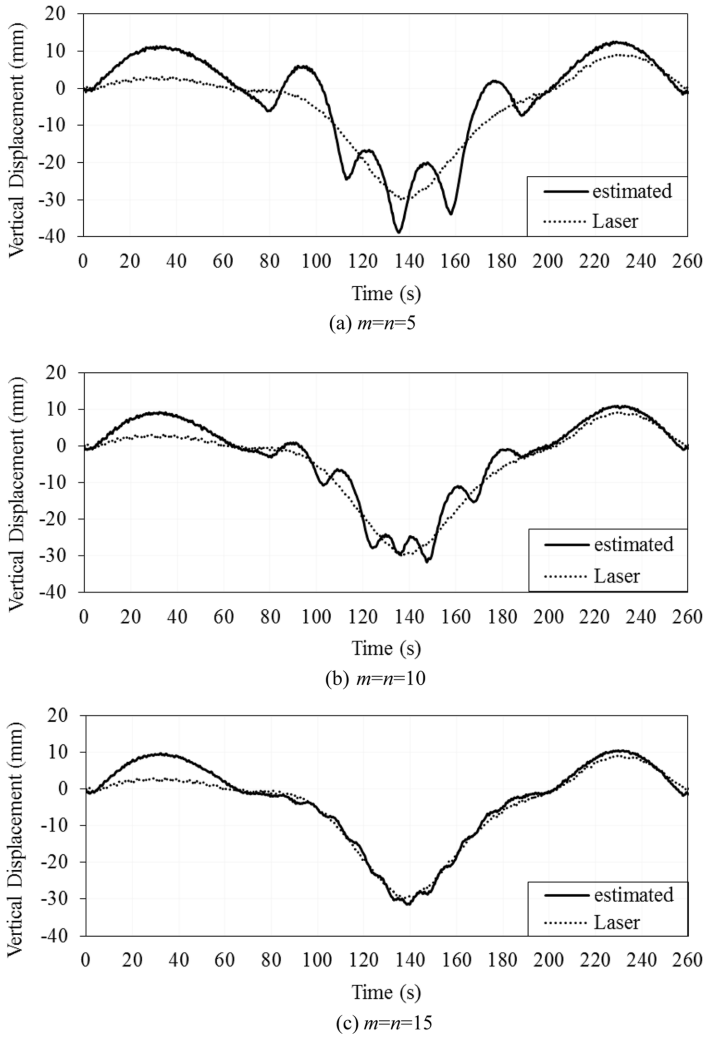

(a) m=n=5

(b) m=n=10

(c) m=n=15

Fig. 10 Effects of the number of FBG sensors on the estimation of vibration displacements

Table 3 Effects of the number of FBG sensors on the estimation results

Number of sensors	Correlation coefficient		Max. Displacement @ midspan		
	Whole	Mid only	u_{est} (mm)	u_{laser} (mm)	Difference (%)
$m = n = 5$	0.9262	0.8819	38.867	29.879	23.13
$m = n = 10$	0.9622	0.9600	31.719		5.80
$m = n = 15$	0.9715	0.9946	31.424		4.92

sensors increases, the estimated vibration displacements approach closer to the measured vibration displacements. Table 3 also verifies the same trend in the estimation results by comparing the correlation coefficients between them. The comparisons indicate that it is necessary to check the proper number of sensors and theoretical mode shapes at the preliminary stage of the measurement plan for a reliable estimation of vibration displacements.

3.3 Application to a multi-girder simple span bridge

The algorithm has also been applied to a five-girder simple span plate-girder bridge. Fifteen FBG sensors were used in total, but only three sensors were placed on each girder as shown in Fig. 11. Five LVDTs were placed at the center of each girder to validate the estimation of vibration displacements. After an initial field test was carried out, it was found that measured data from two

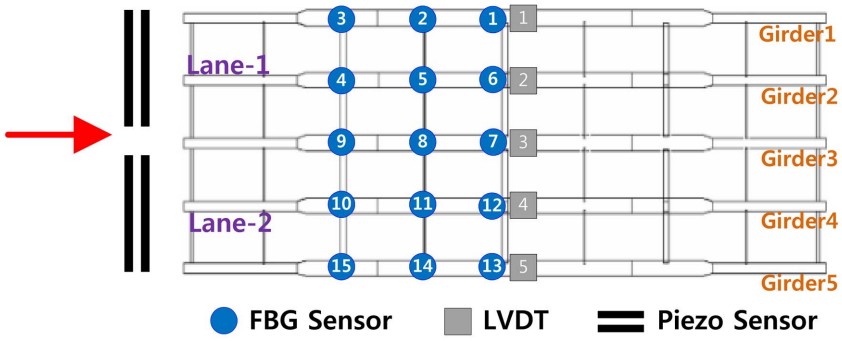

(a) Sensor layout

(b) Trucks for the tests

(c) Girders

Fig. 11 Field test on a simple span plate-girder bridge

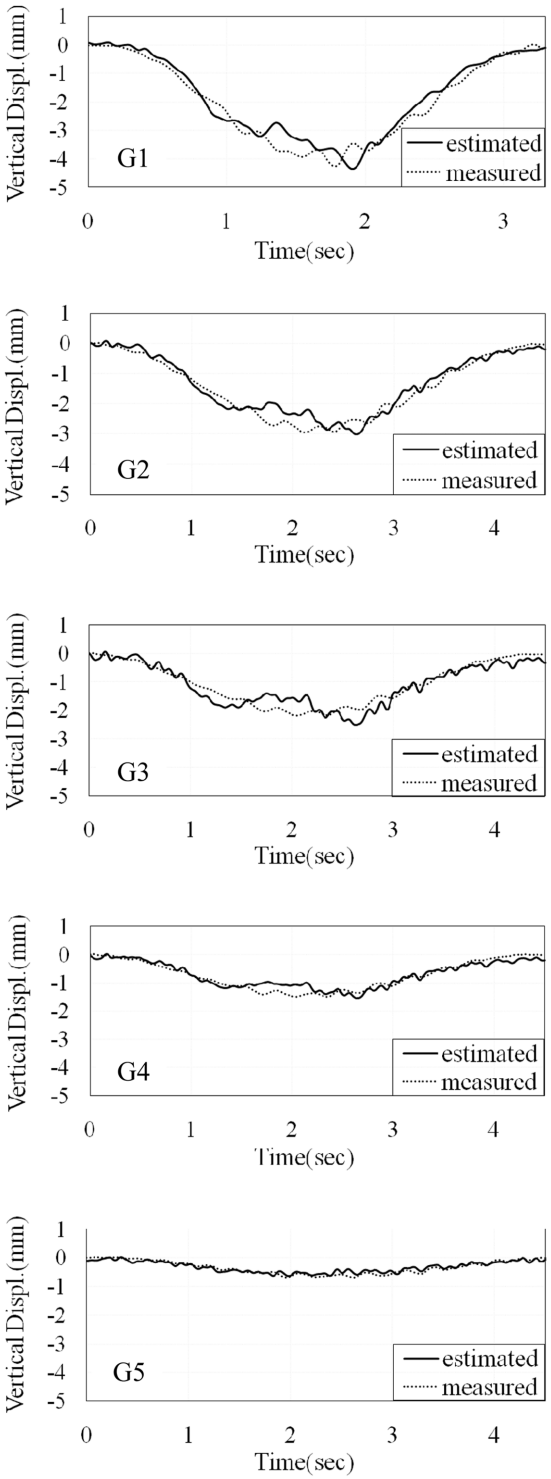

Fig. 12 Comparison of displacements at the center of each girder (load case 3)

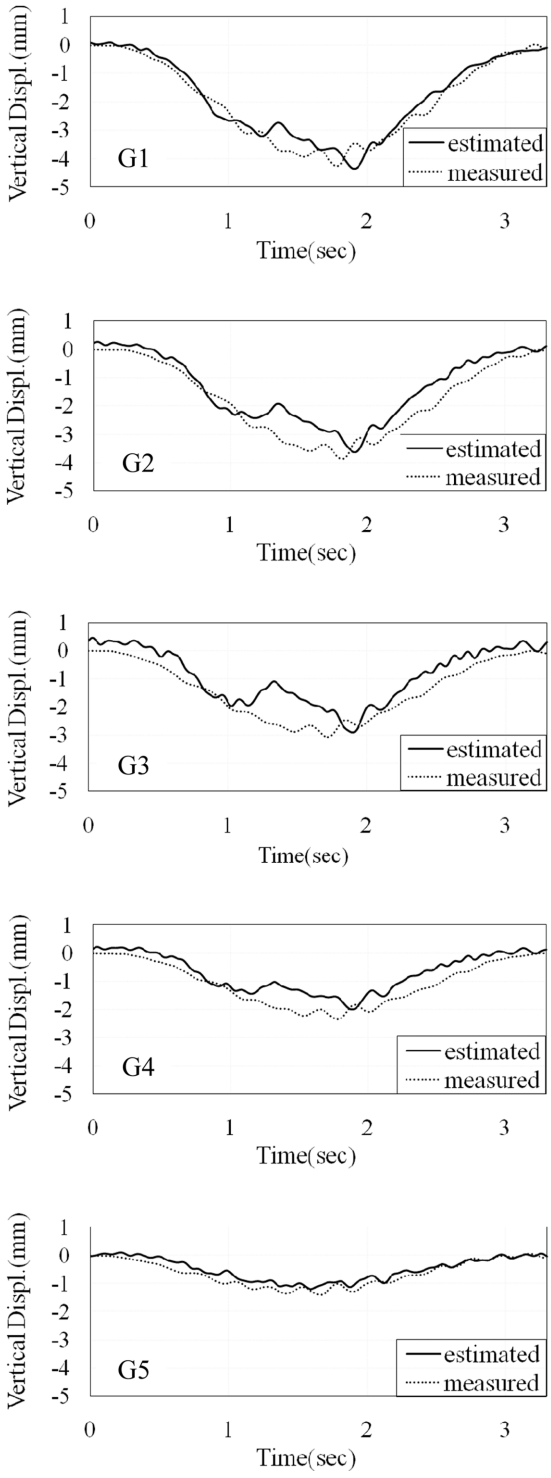

Fig. 13 Comparison of displacements at the center of each girder (load case 6)

FBG sensors of No. 6 and No. 12 fluctuated out of the bound so that the vibration strains at the two locations were replaced by the strains averaged from the adjacent FBG sensors of No. 1, No. 7, and No. 7, No. 13, respectively.

To apply the proposed algorithm, each girder of the bridge was considered as a simply supported beam. The geometric constant y_c was computed as an overall averaged value of y_c from all of the girders. Figs. 12 and 13 compare the measured vibration displacements with the estimated vibration displacements at the midspan of each girder at the speeds of 40 km/hr and 60 km/hr, respectively. Table 4 summarizes the correlation coefficients of each girder for various load cases and Table 5 compares the estimated and measured maximum displacements at the midspan of each girder for the tested load cases.

Table 4 Comparison of correlation coefficients of estimated and measured displacements at the center of each girder for various load cases

Load case	Velocity (km/hr)	Lanes	Correlation coefficient					Average
			G1	G2	G3	G4	G5	
1	5	lane 1	0.984	0.981	0.976	0.976	0.917	0.967
2	5	parallel	0.989	0.978	0.956	0.976	0.990	0.978
3	40	lane 1	0.984	0.970	0.934	0.952	0.950	0.958
4	40	parallel	0.982	0.970	0.952	0.971	0.981	0.971
5	40	10 m serial	0.985	0.892	0.745	0.915	0.988	0.905
6	60	parallel	0.977	0.961	0.932	0.955	0.972	0.959
7	80	10 m serial	0.978	0.896	0.573	0.918	0.977	0.868
Average			0.983	0.950	0.867	0.952	0.968	(0.944)

Table 5 Comparison of maximum displacements at the center of each girder for various load cases

	Load case	1	2	3	4	5	6	7
G1	u_{est} (mm)	1.307	0.942	3.528	4.135	1.651	4.337	1.834
	u_{meas} (mm)	1.362	1.175	3.277	4.115	1.420	4.253	1.716
	Difference (%)	4.02	19.86	7.68	0.49	16.24	1.96	6.85
G2	u_{est} (mm)	1.260	0.911	3.018	3.600	1.823	3.623	1.660
	u_{meas} (mm)	1.109	0.899	2.955	3.735	1.925	3.863	2.192
	Difference (%)	13.58	1.30	2.13	3.62	5.32	6.21	24.29
G3	u_{est} (mm)	1.253	0.880	2.508	3.068	2.301	2.911	1.903
	u_{meas} (mm)	0.796	0.741	2.182	2.985	2.498	3.075	2.751
	Difference (%)	57.36	18.75	14.95	2.77	7.89	5.36	30.82
G4	u_{est} (mm)	0.834	0.669	1.537	2.109	2.466	2.003	2.144
	u_{meas} (mm)	0.606	0.660	1.500	2.292	2.687	2.357	2.942
	Difference (%)	37.52	1.39	2.43	8.01	8.25	15.03	27.11
G5	u_{est} (mm)	0.436	0.471	0.628	1.349	2.844	1.196	2.990
	u_{meas} (mm)	0.255	0.450	0.676	1.398	2.686	1.405	2.897
	Difference (%)	71.00	4.54	7.13	3.47	5.86	14.91	3.20

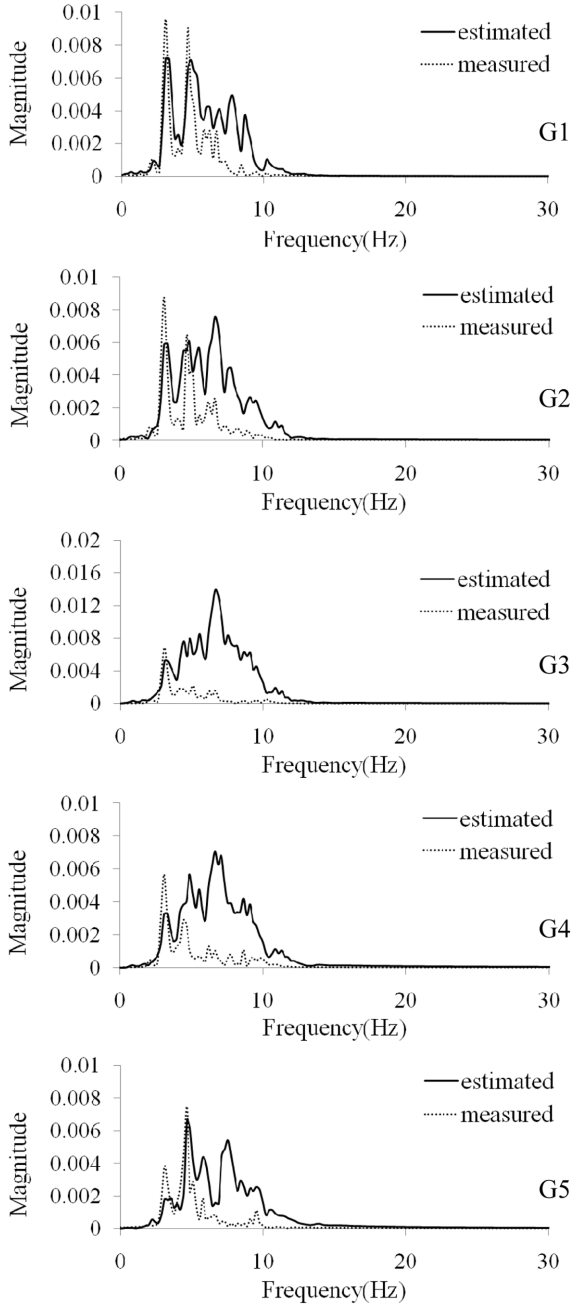

Fig. 14 Comparison of FRFs of displacements at the center of each girder (load case 3)

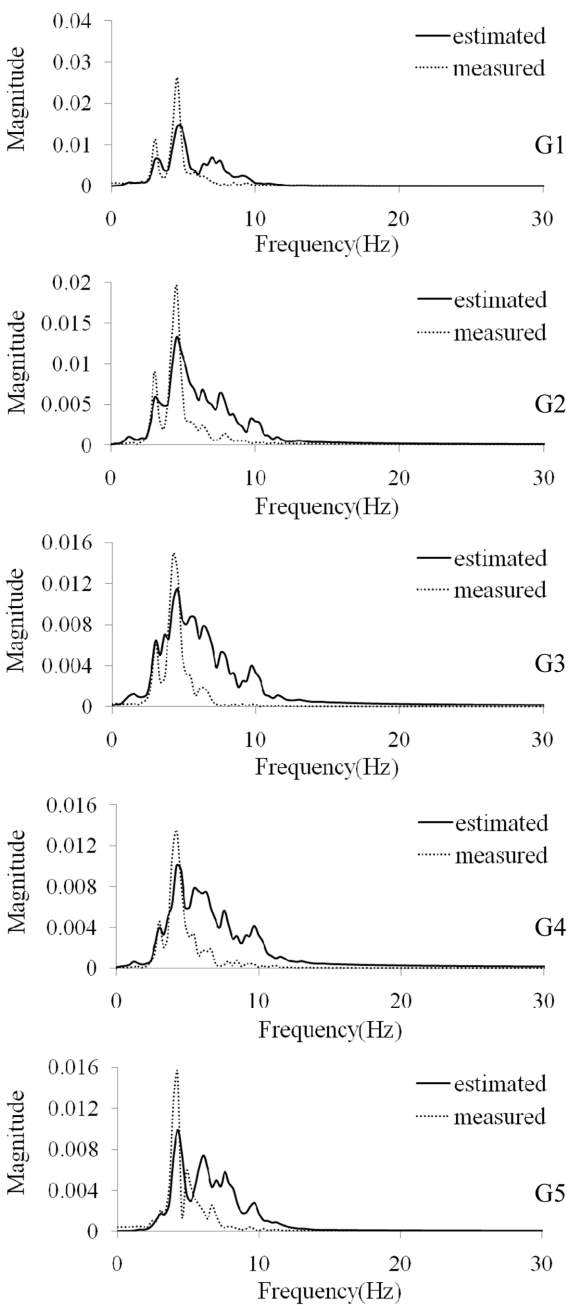

Fig. 15 Comparison of FRFs of displacements at the center of each girder (load case 6)

In Table 5, the largest percentage difference between the estimated and the measured displacements can be found in load case 1. However, the actual magnitude difference is less than 0.5mm. Vertical displacements of the plate-girder bridge in all the cases were very small under the applied load cases as observed in the table. Among the load cases tested, load cases 5 and 7 of two

serial trucks running with a 10 m distance between them provide the worst correlations because the required condition of a 10 m distance with a constant speed was difficult to maintain during the field test. However, most of the displacements of all other cases were reliably estimated.

FRFs of displacements at the center of each girder are compared in Figs. 14 and 15 for different load cases. In all the cases, the peaks in the low frequency range generally match each other well. However, in the slightly higher frequency range, it is observed that all the FRFs of the estimated vibration displacements still have relatively large magnitudes with some peaks. It is believed that this mismatch in the high frequency range can be also improved by using more FBG sensors and thus more theoretical modes. Judging from the application studies of sections 3.1 and 3.2, using more than 5 FBG sensors in each girder could result in better and more reliable estimation of vibration displacements.

4. Conclusions

An algorithm of estimating bridge vibration displacements using measured FBG strain sensors and theoretical beam mode shapes is proposed and has been verified through field tests on various types of bridges. The estimated vibration displacements have been compared by the correlation coefficients, maximum displacements, and also by FRFs. These values and figures proved their usefulness and effectiveness in comparing vibration displacements. In the current approach, the number of theoretical modes for estimating vibration displacements has been selected to be the same as the number of FBG sensors used for a field test.

To apply the proposed algorithm for an actual bridge, a geometric constant needs to be selected. Theoretically, the geometric constant can be computed from the given sectional information of a bridge. However, since the beam theory cannot be exactly satisfied in an actual structure, it is proposed in the current approach that the geometric constant is rather determined as a scale factor from a controlled field test with a truck running at a low speed. However, after the geometric constant is determined once, it can be used afterwards without revising it.

For all the tested cases with different types of bridges, the estimated vibration displacements from the proposed algorithm have agreed relatively well with the directly measured vibration displacements. The application to a plate-girder bridge with multi girders showed relatively worse results compared with the other cases but this demonstrates that a proper number of FBG sensors should be used for each girder to estimate vibration displacements accurately. Therefore, it is recommended that a proper number of FBG sensors should be determined at the preliminary stage of the measurement plan.

The proposed method can be also applied to any other type of structures whose theoretical mode shapes can be obtained and strains are reliably measured at sufficient locations.

Acknowledgements

This research was supported by a grant of KICTEP 08-E01 from the Super Long Bridge R&D Center and also by an INHA UNIVERSITY Research Grant. The authors are grateful to Dr. Seong-Il Kim and Dr. Won-Seok Chung of KRRI for allowing the use of the field test data from the bridge for a Maglev train.

References

AASHOTO (2008), The Manual for Bridge Evaluation.

Bhagwat, M., Sasmal, S., Novák, B. and Upadhyay, A. (2011), "Investigations on seismic response of two span cable-stayed bridges", *Earthq. Struct.,* **2**(4), 337-356.

Brownjohn, J., Rizos, C., Tan, G.H. and Pan, T.C. (2004), "Real-time long-term monitoring of static and dynamic displacements of an office tower, combining RTK GPS and accelerometer data", *Proceedings of the 1st FIG International Symposium on Engineering Surveys for Construction Works and Structural Engineering*, **1**(TS1.9), 1-15.

Chan, T.H.T., Ashebo, D.B., Tam, H.Y., Yu, Y., Chan, T.F., Lee, P.C. and Gracia, E.P. (2009), "Vertical displacements measurements for bridges using optical fiber sensors and CCD cameras - a preliminary study", *Struct. Hlth. Monit.,* **8**, 243-249.

Chang, S.J., Kim, N.S. and Kim, H.K. (2009), "Prediction of displacement response from the measured dynamic strain signals using mode decomposition technique", *Proceedings of the ICOSSAR 2009 The 10th International Conference on Structural Safety and Reliability*, Japan.

Davis, M.A., Kersey, A.D., Sirkis, J. and Friebele, E.J. (1994), "Fiber Optic Bragg Grating Array for Shape and Vibration Mode Shape Sensing", SPIE 2191, 94-101.

Foss, G.C. and Haugse, E.D. (1995), "Using Modal Test Results to Develop Strain to Displacement Transformations", *Proceeding of the 13th International Modal Analysis Conference*, 112-118.

Gindy, M., Vaccaro, R., Nassif, H., and Velde, J. (2008), "A state-space approach for deriving bridge displacement from acceleration", *Comput.-Aid. Civil Infrastr. Eng.*, **23**(4), 281-290.

Inaudi, D., Conte, J.P., Perregaux, N. and Vurpillot, S. (1998), "Statistical analysis of under-sampled dynamic displacement measurement", *SPIE Smart Structures and Materials*, **3325**, San Diego.

Jiang, J., Lu, X. and Guo, J. (2002), "Study for real-time monitoring of large-span bridge using GPS", *Proceedings of ISSST 2002, Progress in Safety Science and Technology*, 308-312.

Jung, B.S. and Kim, N.S. (2006), "Assessment of the dynamic displacements using acceleration data measured on bridge superstructures", *Proceedings of the 3rd International Conference on Bridge Maintenance*, *Safety and Management*, Portugal.

Kang, L.H., Kim, D.K. and Han, J.H. (2007), "Estimation of dynamic structural displacements using fiber Bragg grating strain sensors", *J. Sound Vib.*, **305**, 534-542.

Kirby, G.C., Lim, T.W., Weber, R., Bosse, A.B., Povich, C. and Fisher, S. (1997), "Strain-based shape estimation algorithms for a cantilever beam", SPIE 3041, 72-81.

Lassif, H.H., Gindy, M. and Davis, J. (2005), "Comparison of laser doppler vibrometer with contact sensors for monitoring bridge deflection and vibration", *NDT&E Int.*, **38**, 213-218.

Lee, J.J., Fukuda, Y. and Shinozuka, M. (2006), "Dynamic displacement measurement of bridges using vision-based system", *Proceedings of SPIE, International Society for Optical Engineering*, **6174**(2), 1-9.

Liu, J., Zhu, S., Xu, Y. and Zhang, Y. (2011), "Displacement-based design approach for highway bridges with SMA isolators", *Smart Struct. Syst.*, **8**(2), 173-190.

Meng, X., Dodson, A.H. and Roberts, G.W. (2007), "Detecting bridge dynamics with GPS and triaxial accelerometers", *Eng. Struct.*, **29**, 3178-3184.

Park, K.T., Kim, S.H., Park, H.S. and Lee, K.W. (2005), "The determination of bridge displacement using measured acceleration", *Eng. Struct.*, **27**, 371-378.

Shin, S., Han, M.J., Jo, J.Y., Lee, H.J. and Jung, B,S. (2007), "Identification of moving forces by measuring bridge dynamic responses", *Proceedings of the 3rd International Conference on SHM of Intelligent Infrastructures*, China

Todd, M.D., Johnson, G.A., Chang, C.C. and Malsawma, L. (2000), "Real-time girder deflection reconstruction using a fiber Bragg grating system", *Proceedings of the International Modal Analysis Conference XVIII,* San Antonio, Texas, February.

Todd, M.D. and Vohra, S.T. (1999), "Shear deformation correction to transverse shape reconstruction from distributed strain measurements", *J. Sound Vib.*, **225**(3), 581-594.

Vohra, S.T., Johnson, G.A., Todd, M.D., Danver, B.A. and Althouse, B.A. (2000), "Distributed strain monitoring with arrays of fiber Bragg grating sensors on an in-construction steel box-girder bridge", *IEICE Transactions*

on Electronics, **E83-C**(3), 454-461.
Vurpillot, S., Inaudi, D. and Scano, A. (1996), "Mathematical model for the determination of vertical displacement from internal horizontal measurements of a bridge", *Smart Systems for Bridges, Structures, and Highways*, **3043**.
Whiteman, T., Lichti, D.D. and Chandler, I. (2002), "Measurement of deflections in concrete beams by close-range digital photogrammetry", *Symposium on Geospatial Theory, Processing and Application*.